Title
Multiple-Peak Response to Tracer Injection Tests in Single Fractures: A Numerical Study

Journal
Water Resources Research, 27(8)

Authors
Moreno, L.
Tsang, C.F.

Publication Date
1991

LBL-30360
Preprint

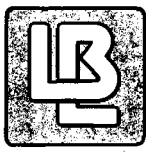

Lawrence Berkeley Laboratory
UNIVERSITY OF CALIFORNIA

EARTH SCIENCES DIVISION

Submitted to Water Resources Research

Multiple-Peak Response to Tracer Injection Tests in Single Fractures: A Numerical Study

L. Moreno and C.-F. Tsang

January 1991

Prepared for the U.S. Department of Energy under Contract Number DE-AC03-76SF00098

DISCLAIMER

LBL-30360

Multiple-Peak Response to Tracer Injection Tests in Single Fractures: A Numerical Study

Luis Moreno[*] *and Chin-Fu Tsang*[†]

[*]Department of Chemical Engineering
Royal Institute of Technology
S-100 44 Stockholm, Sweden

[†]Earth Sciences Division
Lawrence Berkeley Laboratory
University of California
Berkeley, California 94720

January 1991

This work was supported jointly by the Director, Office of Civilian Radioactive Waste Management, Office of Facilities Siting and Development, Siting and Facilities Technology Division, of the U.S. Department of Energy under Contract No. DE-AC03-76SF00098, and by the Swedish Nuclear Fuel Company, Stockholm, Sweden.

ABSTRACT

Under certain conditions, when pulse tracer injection tests are performed in a single fracture with a regional flow field, the breakthrough curves may display multiple peaks. Furthermore the shape of these curves may change when the injection flowrate is varied. In this paper the conditions under which the breakthrough curve may present multiple peaks are analysed numerically using stochastically generated fractures. The dispersivities of these peaks are also calculated. It is found that the dispersivity is small for each of the peaks and that the dispersivities of the different peaks in a breakthrough curve are quite similar. The results presented in this paper may be equally applied to tracer tests in a two-dimensional strongly heterogeneous medium.

INTRODUCTION

In experimental tracer tests carried out in a single fracture zone in crystalline rock, the breakthrough curves obtained using pulse tracer injection have multiple peaks in some situations (Hadermann, 1989; Hoehn et al.,1989; Steffen and Steiger, 1988). In some cases, it is observed that the shape of these breakthrough curves changes when the injection flowrate is varied. Moreover, the behavior of these multi-peaked curves is observed only for a limited range of injection flowrates.

Moreno et al. (1988) have presented a two-dimensional stochastic model for flow and solute transport in a fracture with variable apertures. The results show that the fluid flows unevenly in a single fracture and that it takes place in preferred paths. In a subsequent study (Moreno et al., 1990) we modified the model to allow for point solute injection and withdrawal in the two-dimensional fracture plane.

In this paper, some recent simulations of tracer tests in a single fracture with variable apertures are presented. The aim is to study the conditions under which the breakthrough curve may present multiple peaks. We will also study how the injection flowrate modifies the shape of the curves in different situations. While the study is focussed on multiple peaks observed during tracer test with pulse injection, the results can be applied to the case of continuous injection. The breakthrough curve for the latter case would show multiple steps, where each step corresponds to the arrival of a pulse in the pulse test.

DESCRIPTION OF THE MODEL

The apertures of a fracture are not constant in magnitude but vary spatially in the fracture plane. Fluid flowing through the fracture seeks out the least resistive pathways. The main flow is expected to occur through a few channels in the fracture plane (Abelin et al., 1985, Neretnieks, 1987). In defining channels, we mean preferred flowpaths in the fracture. If the direction of the pressure gradient is changed then a new pattern of channel network would be obtained (Tsang and Tsang, 1989). Though the pattern of channel networks are dependent on pressure gradients, Tsang and Tsang (1989) demonstrated that they can be characterized stochastically by the same set of parameters as long as the anisotropy of the spatial correlation of the apertures remains relatively small.

Let us assume that we have a fracture with an overall flow under a "regional" pressure gradient. A solution containing the solute is then injected with a given flowrate at a point in the fracture plane. The injection pressure increases the local pressure profile and hence modifies the original fluid flow pattern around the

injection point. For a given distribution of the variable apertures, the injection feeds the solute into flow paths that are in the neighborhood of the injection point. The larger the injection flow, the larger will be the local pressure profile and the larger the number of paths which may be reached by the solute. However, the pattern of these flow paths depends strongly on the variable apertures near the injection point.

More specifically, generation of the spatial distribution of fracture apertures is performed by partitioning the fracture by grids with a different aperture assigned to each node enclosed by grid lines. The aperture values used are defined by an aperture density distribution (mean aperture b = 80 μm and spread σ_{lnb} = 0.5) and a spatial correlation length (λ/L = 0.1). A lognormal distribution for these apertures and an exponential function for the spatial covariance of the apertures were chosen. Details may be found in Moreno et al (1988). For the present study the grid is 40 x 40 nodes. An example of the generated variable-aperture fracture is shown in Figure 1.

Now let us locate a production well with pumping flowrate Q, at the upper-right corner of the square shown in Figure 1. We may assume that this represents a quarter of the fracture plane with a production well at its center. Then by symmetry, upper and right boundaries are made closed boundaries and left and lower boundaries are constant-pressure boundaries. The model is an approximation to a case of convergent tracer test in a fracture where the production well may be a drift where tracer is collected, such as the MI experiment carried out at Grimsel, Switzerland (Hoehn et al., 1989). The location of an tracer injection well, with injection rate q, may be chosen at different points in the fracture plane, and in Figure 1, it is defined by the index (n_x,n_y) of the respective node, where n_x and n_y are between 1 and 40. Typically q is much less than Q.

Fluid flow is then calculated assuming that it is proportional to the cube of the aperture at each node. We assumed the apertures are very much smaller than the flow distance in the nodes, so that the influence on pressure drop by the diverging or converging parts of the flow path is negligible. From the fluid balance in each node, the pressure at each node is calculated.

The solute transport is simulated using a particle-tracking technique (Schwartz et al., 1983; Robinson, 1984; Moreno et al., 1988, 1990). Six thousand particles are introduced in the flow field at the injection node. Each particle is then followed along its path from the injection to the collection point through the intersections The particle tracking method used considers no mixing at these intersections. However within each branch in between adjacent intersections, perfect mixing is assumed (See Moreno et al., 1990). Note that the method includes an intrinsic transverse dispersivity equal to grid size due to numerical dispersion.

The residence time of an individual particle over the whole path in the fracture plane is determined as the sum of residence times in all the steps that the particle has traversed. The residence time distribution is then obtained from the residence times of a multitude of individual particle runs.

RESULTS OF THE SIMULATIONS

Flow and solute transport for these different fractures were calculated. These are generated based on the same fracture aperture probability density function and spatial correlation length. Thus they are actually three different realizations out of the same statistical input parameters.

With the production well (See Figure 1) maintained at flowrate Q, tracer injection in a single fracture is simulated for different injection locations and flowrates. For each case, flow paths, solute paths, and breakthrough curves are calculated and plotted. The injection flowrate q is first varied over a wide range (0 to 3 % of Q) to determine the interval within which the shape of the breakthrough curves is sensitive to this value. When this interval is found, additional calculations are performed using flowrates within this interval to study in detail the breakthrough curves as a function of flowrates.

In preliminary simulations, we also studied the tracer breakthrough curve as a composite of several partial breakthrough curves, each of which is due to transport of tracer particles through different specified areas in the fracture plane between the injection and collection points. We have computed a number of such partial breakthrough curves. It was found that for most cases when the total breakthrough curve observed at the collection hole possesses multiple peaks, the partial curves are found also to display multiple peaks. We also noticed that the shape of the curves is predominately influenced by the condition around the injection point.

The characteristics of the area around the injection point that may be of interest to study would be: the nearby fracture apertures, the existence (or nonexistence) of paths with a large flowrate close to the injection point, and the pressure distribution around the injection point.

Large fracture apertures around the injection point may imply large residence times at this location. On the other hand, small apertures may cause the injected tracer to be dispersed around the injection point.

The existence of paths of large flow close to the injection point would permit a great

proportion of the tracer flow into these paths. On the other hand if there are no paths of large flow close to the injection point, the solute has to seek some small and slow paths to flow to the collection hole. The travel times may then be very different from each other, thus resulting in breakthrough curves having multiple peaks.

The pressure distribution around the injection hole is a function of the injection flowrate and determines the major directions in which the solute would start to flow from the injection point. For small injection flowrates, the solute flows in the water pattern originally established prior to solute injection. With increasing injection flowrate, however, flow tends to flow radially from the injection point and, in particular, flow in directions opposite to the direction towards the collection point is also possible.

Results for fracture 1.

For the first of the three fractures chosen for our study, the flow paths are shown in Figure 2 for a negligible injection flowrate. The majority of water flow occurs in a few paths or channels to the collection hole, as discussed above.

For injection at the location (n_x,n_y) = (15,15), the breakthrough curves show one peak for injection flowrates from negligible to 1.0 % of the total flowrate Q in the fracture. When the injection flowrate is increased from 0.01 Q to 0.025 Q the breakthrough curves change from one peak to two main peaks. For a flowrate of 0.025 Q, the curve shows several small peaks at large residence times. Breakthrough curves for different injection flowrates are shown in Figure 3. The travel time for the first peak does not change with the injection flowrate.

For the small injection flowrate at (15,15), most of the injected solute flows to the collection hole through the same paths. When flowrate is increased the number of paths involved in tracer transport is greatly increased. This is shown in Figure 4. In this figure, we note that for a small injection flowrate most of the solute flows to the right from the injection point, and only a small amount flows down and up. When the flowrate is increased the fraction of solute which flows to the left is strongly increased. This fraction is increased from 0.5 to 35.6 % for injection flowrates increasing from 0.01 Q to 0.025 Q. It is this part of the injected solute (tracer particles) that creates several new paths around the injection point and give rise to the second peak observed in the breakthrough curve for large flowrates. The influence of particles which move down is small.

The above observations were further illustrated by calculating four partial breakthrough curves by requiring that the tracer particles are those that flowed

from the injection points in the up, down, left, or right directions respectively. Such calculations were done for different injection flowrates. The results for the partial breakthrough curve of particles flowing to the left of the injection point are shown in Figure 5 and compared with the total breakthrough curve. Similar results are obtained for the other partial breakthrough curves.

Results for fracture 2

The water flow pattern in fracture 2 is shown in Figure 6. For this fracture simulations were performed for two alternative injection locations, designated by (n_x,n_y) = (15,15) and (n_x,n_y) = (8,8).

For injection at the point (15,15), the breakthrough curves show only one peak for injection flowrates varying over a wide interval. This could be explained by the fact that injection occurs at a location with large flow and is thus well connected to main flow paths of the fracture. For this reason the same paths are available for the solute transport regardless of the injection flowrates.

For injection at the point (8,8), which is in a low flow velocity region, breakthrough curves have two peaks for injection flowrate varying from 0.01 Q to 0.03 Q. These curves are shown in Figure 7. As the flowrate is increased the first peak grows. For the larger flowrate, the second peak is small and additional small peaks appear at long residence times as well. Both the two main peaks are shifted to shorter residence times when the injection flowrate is increased. This latter result indicates that for small injection flowrate the residence time around the injection point is large and it decreases with increasing injection flowrate. The patterns for the transport of the solute for the large and small flowrate are different only around the injection hole.

The partial breakthrough curves obtained for the solute which flows initially in the four different directions from the injection point all show two peaks for the range of flowrates used in these simulations. These partial peaks are also shifted to the shorter travel times and their relative size is varied with increasing flowrate.

Results for fracture 3

The water flow paths for fracture 3 with a negligible injection flowrate are shown in Figure 8. For this fracture simulations were performed for three injection locations: (n_x,n_y) given by (15,15), (11,11), and (8,8) respectively.

For injection at (15,15), the breakthrough curves show only one peak for the range

of injection flowrates used in the simulations (0.003 Q to 0.03 Q). The tails of the breakthrough curves increase with increasing injection flowrates. This could be explained as follows. Original flow at the injection point is small. But the injection point is located close to a path with enough good connection to the collection hole. Thus as flowrate increases, more and more solute feeds into this channel, giving rise to the longer tail.

The breakthrough curves for injection at (11,11) show one peak over the whole range of injection flowrates used (from 0.001 Q to 0.03.Q). The fracture apertures around the injection point are large and the flow in the injection point is also large. Then the patterns for the solute transport are similar, regardless of the injection flowrates used in the simulations.

For injection at (8,8), the breakthrough curve shows one peak for flowrates smaller than 0.003 Q. When the flowrate is increased beyond this value a new peak starts to build up at a shorter residence time and the previous peak is reduced. For an injection flowrate of 0.03 Q, the peak at the short residence time is larger than the peak at the longer residence time. This variation of the relative sizes of the peaks is shown in Figure 9. The patterns of the solute transport are shown in Figure 10. For an injection flowrate of 0.01 Q new transport paths are created near the injection point, but the solute paths farther away are similar to those at lower flowrates. When the flowrate is increased even more, new paths are formed and new areas away from the injection point are involved in solute transport (Figure 10)

Determination of Dispersivity.

In our calculations, we have assumed that dispersion is mainly determined by different velocities in the different pathways, i.e., channeling dispersion. For a breakthrough curve with two peaks, we may assume that the solute flows through two main groups or channels of flow paths with different travel times. In each peak or channel, we assume a group of flow paths with similar velocities that can be represented by a certain hydrodynamic dispersion term. This dispersion is determined by the width of the peak in the breakthrough curve.

A way to estimate the dispersion of the breakthrough curve is by determining the ratio between the width of the pulse and the time at the peak maximum. The width of the pulse is determined at a concentration of 50 % of the peak concentration. The relationship between this ratio and the Peclet number and hence the dispersivity may be obtained from the solution of Lenda and Zuber (1970) for pulse injection. The calculated dispersivities for fracture 2 and fracture 3 using this method are shown in Table 1.

Two interesting observations may be made from Table 1. First, all the dispersivity values for the peaks are very small compared with the transport distance L. However a composite dispersivity value obtained by analysis of all the peaks together will be much larger. Secondly, within a factor of two, these small dispersivity values are similar for the two peaks and for the two fractures and independent of injection flowrates. This may be the consequence that both fractures obey the same aperture probability distribution function.

Note that in in-situ tracer tests the peaks observed could show a larger spreading because of other factors which may cause dispersion, such as, dispersion within each flow path, dispersion due to matrix diffusion, and dispersion in the injection and collection devices. These dispersion effects cause the observed breakthrough curves to be more spread out and the peaks may be less clearly defined.

SUMMARY OF THE RESULTS

From the results of our simulations presented above, we may distinguish the following cases of injection tracer tests:

- If the injection occurs on a main flow channel in the fracture plane, the breakthrough curve would possess a single peak. This peak is almost independent of the injection flowrate.

- If the injection does not occur on a main flow channel, multiple peaks may be observed.

- Dispersion depends on the numbers of possible paths near injection point.

In the case where the injection does not occur on a main flow channel, we may distinguish three possible alternative cases:

- A time shift of the first peak with a variation of the injection flowrate: the residence time decreases with an increase of the injection flowrate.

- When the injection flowrate is increased, the magnitude of the first peak decreases and the second peak builds up. Additional small peaks for long residence times may also emerge.

- Alternatively, when the injection flowrate is increased, the magnitude of the first peak increases.

The dispersivity values determined for the peaks in a multiple-peak tracer

breakthrough curve are expected to be similar and small in magnitude. In practical field measurements, the observed dispersivity may in some cases be dominated by other dispersive processes. On the other hand, if the peaks are analyzed together as a single breakthrough curve, the dispersivity value obtained will be much larger.

The discussions and results presented in this paper may equally apply to tracer tests in a two dimensional strongly heterogeneous medium. While there are differences in permeability-porosity relationships between fractured and porous media, we expect that qualitatively the multiple-peak tracer transport behavior as discussed here should also be expected in such heterogeneous porous medium systems.

ACKNOWLEDGEMENTS

The main impetus motivating the present paper came out of a number of discussions on recent field data on tracer transport in a single fracture with Jörg Hadermann, to whom we are most grateful. We would also like to acknowledge continued discussion and cooperation with Y.W. Tsang and I. Neretnieks. Review and comments on the manuscript by Jörg Hadermann, J. Noorishad and Y.W. Tsang are appreciated. Work is jointly supported by Swedish Nuclear Fuel Company, Stockholm, Sweden, and the Office of Facility Siting and Developments, Siting and Facilities Technology Division, Office of Civilian Radioactive Waste Management, U.S. Department of Energy under contract number DE-AC03-76 SF 00098 with LBL.

REFERENCES

Abelin, H., I. Neretnieks, S. Tunbrant, and L. Moreno, Final Report of the Migration in a single fracture, experimental results and evaluation, Stripa Project, Tech. Rep 85-03, Nuclear Fuel Safety Project, Stockholm, Sweden, 1985.

Hadermann, J., Private communication, Paul Scherrer Institute, Switzerland, 1989.

Hoehn, E., U. Frick and J. Hadermann, A radionuclide migration experiment in fractured granitic rock, Intern. Symp. on Process governing the movement and fate of contaminants in the subsurface environment, Stanford, CA, July 24-26, 1989.

Lenda, A., and A. Zuber, Tracer dispersion in ground water experiments, Proceedings of a symposium organized by IAEA, Vienna, 1970.

Moreno, L., Y. W. Tsang, C. F. Tsang, F. Hale, and I. Neretnieks, Flow and transport in a single fracture: a stochastic model and its relation with field observations, Water Resour. Res, 24(12), 2033-2048, 1988.

Moreno, L., C. F. Tsang, Y. Tsang, and I. Neretnieks, Some anomalous features of flow and solute transport arising from fracture aperture variability, Water Resour. Res., 26(10), 2377-2391, 1990.

Neretnieks, I., Channeling effects in flow and transport in fractured rocks - some recent observations and models. Swedish Nuclear Power Inspectorate, Proceedings of GEOVAL-87, Stockholm, Sweden, 1987.

Robinson, P. C., Connectivity, flow and transport in network models of fractured media, Ph.D. Thesis, Oxford University, Oxford, 1984.

Schwartz, F. W., L. Smith, and A. S. Crowe, A stochastic analysis of macroscopic dispersion in fractured media, Water Resour. Res., 19(5), 1253-1265, 1983.

Steffen, P., and H. Steiger, NAGRA Felslabor Grimsel, Migration, Traceruntersuchungen, Vorversuche 1-4, GEMAG (Aktiengesellschaft für Geologisch-Physikalische Messungen), Alberswil, Switzerland, 1988.

Tsang, C. F., A new approach to tracer transport analysis: from fracture systems to strongly heterogeneous porous media, Proceeding, International Workshop on Appropriate methodologies for development and management of groundwater resources in developing countries, Hyderabad, India, Feb 28-March 4, Vol 3, 199-222, Oxford & IBH Publishing Co., New Delhi, 1989.

Tsang, Y. W., and C. F. Tsang, Flow channeling in a single fracture as a two dimensional strongly heterogeneous permeable media, Water Resour. Res., 25(9), 2076-2080, 1989.

Table 1. Dispersivity values calculated from the width of the peak in the breakthrough curve.

Curve	1st peak	2nd peak
Fracture 2 (Injection at (8,8))	Dispersivity/L	
q/Q = 0.001	0.0060	0.0030
q/Q = 0.003	0.0059	0.0035
q/Q = 0.01	0.0049	0.0039
q/Q = 0.03	0.0044	0.0032
Fracture 3 (Injection at (8,8))	Dispersivity/L	
q/Q = 0.01	0.0028	0.0037
q/Q = 0.02	0.0033	0.0042
q/Q = 0.03	0.0059	0.0078

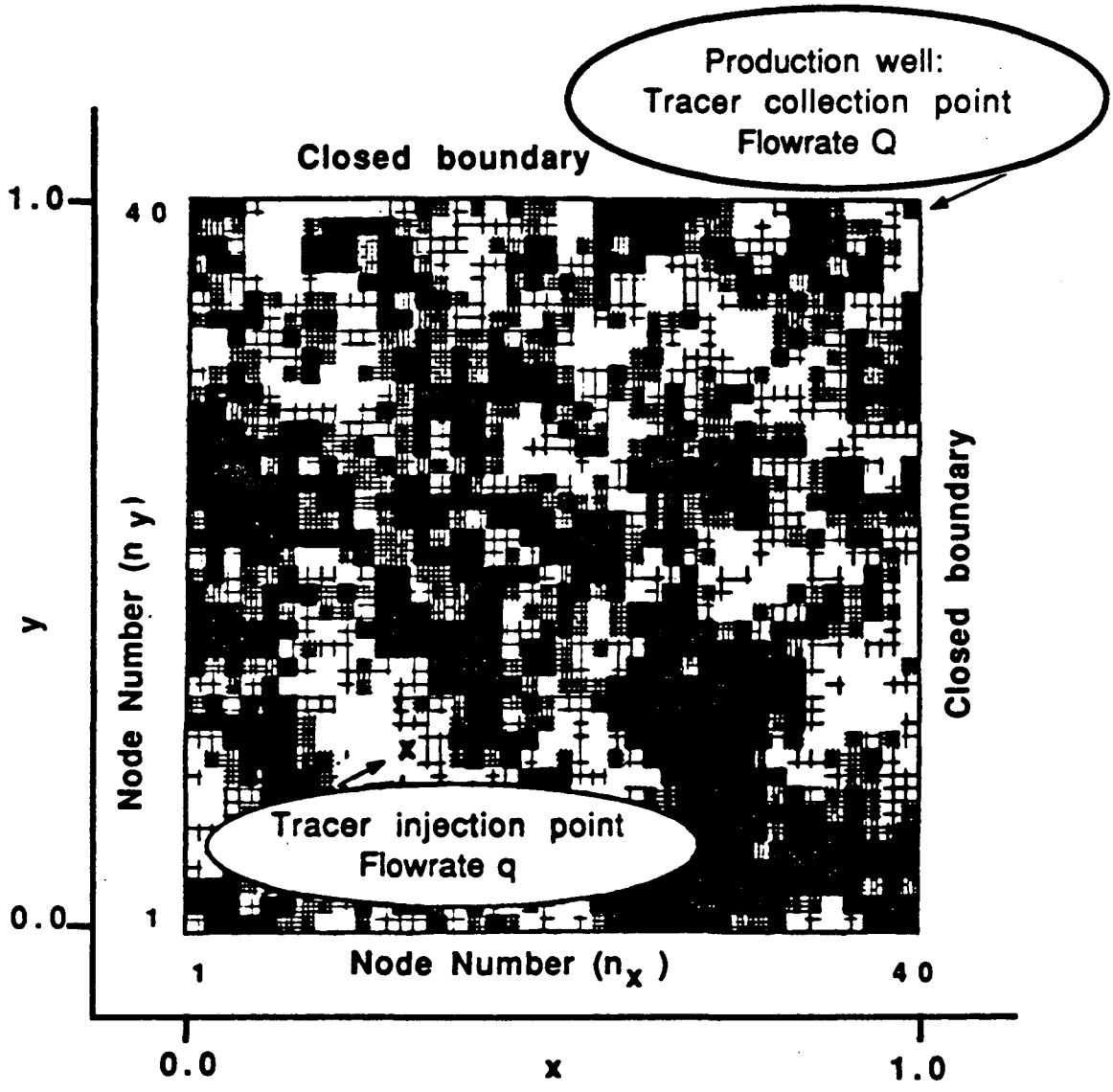

Figure 1 One realization of variable-aperture fracture. A typical tracer injection point (with injection flowrate q) is marked by "x". The top and right hand-side boundaries are closed, and the bottom and left hand-side boundaries are maintained at a constant pressure relative to the production well.

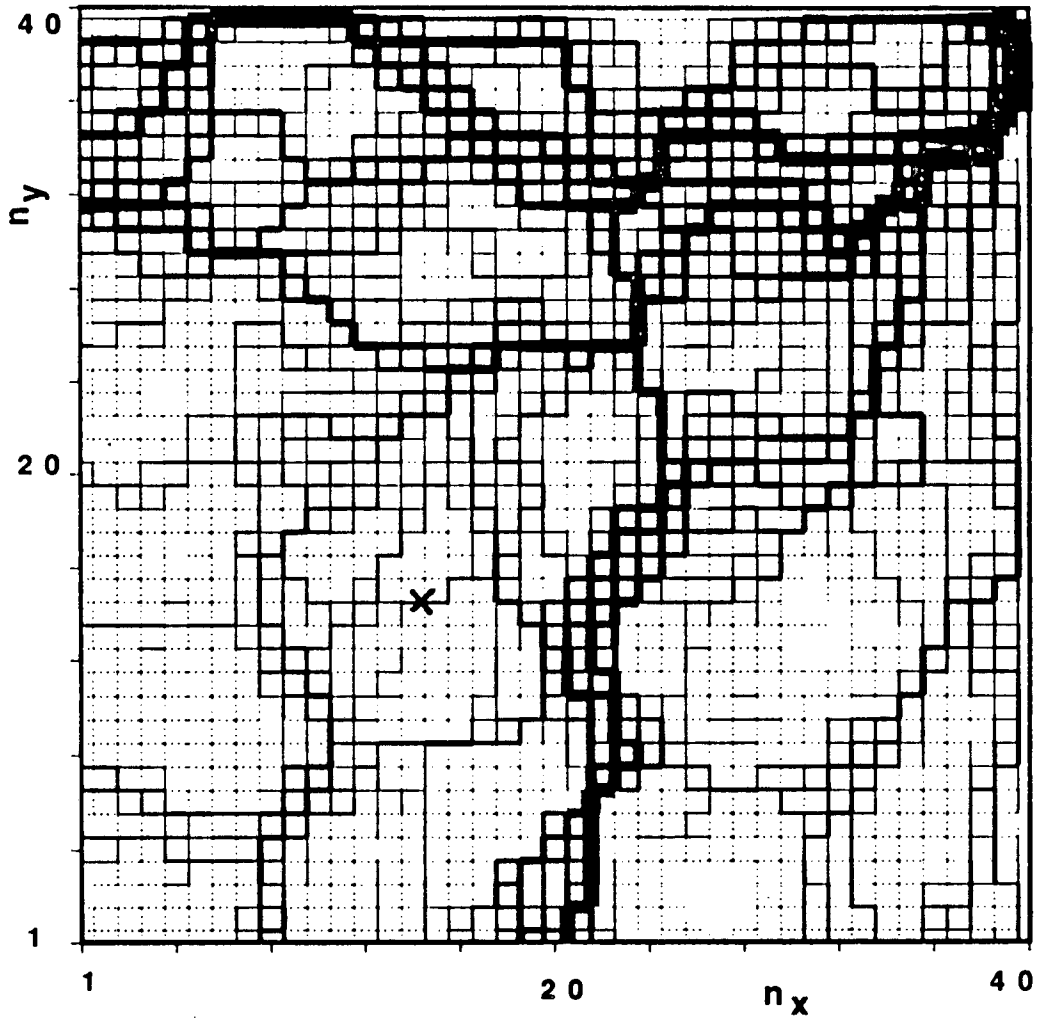

Figure 2 Flow paths in fracture 1 for a negligible injection flowrate. The injection point ("x") is (15,15).

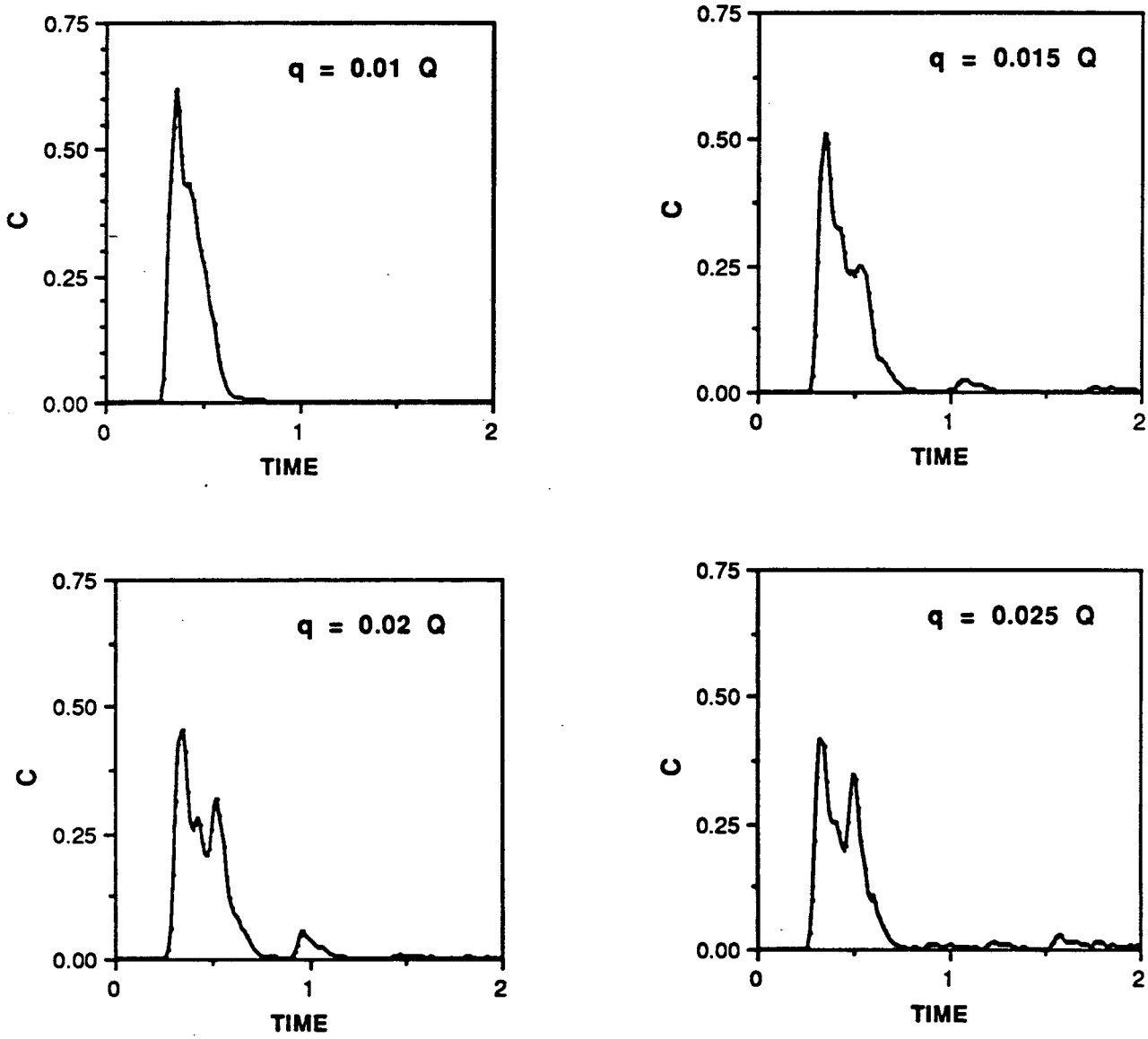

Figure 3 Breakthrough curves for fracture 1, for injection flowrate of 0.01 Q, 0.015 Q, 0.02 Q, and 0.025 Q. Injection at (15,15).

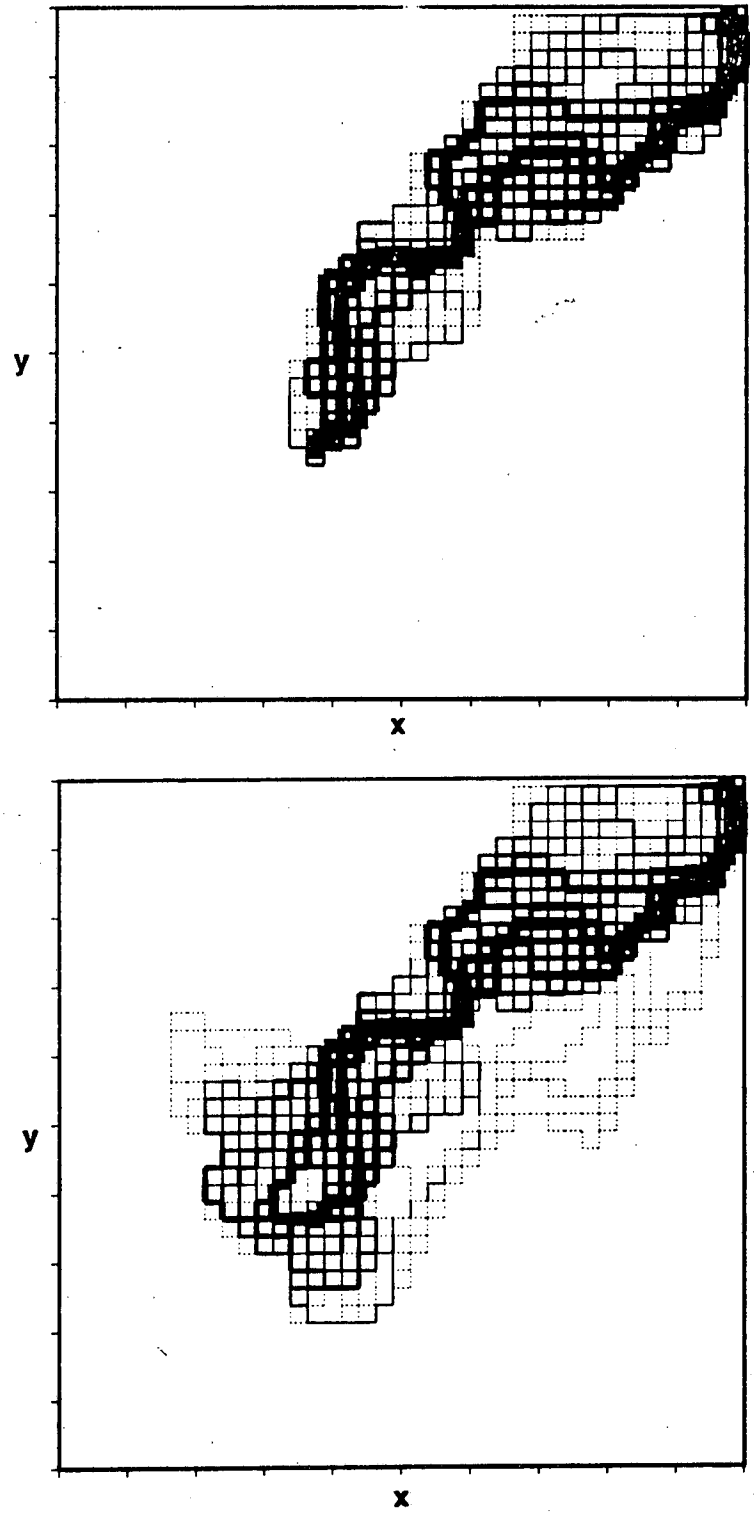

Figure 4 Tracer paths in fracture 1 for injection flowrate of 0.01 Q and 0.025 Q. Injection at (15,15).

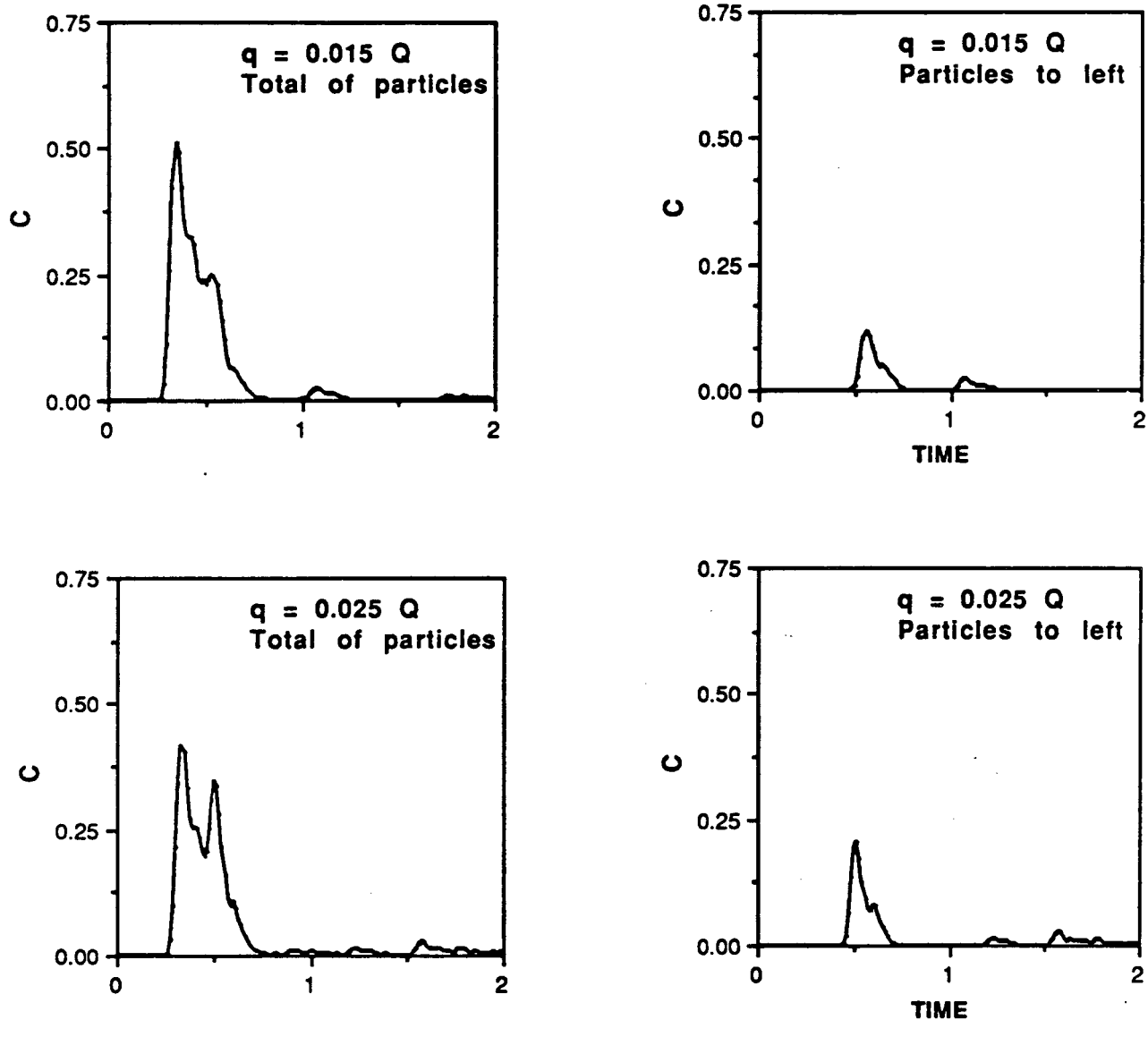

Figure 5 Breakthrough curves in the collection hole for the total of the particles and for the particles that first flow to the left the injection hole. For injection flowrate of 0.01 Q and 0.025 Q. Injection at (15,15).

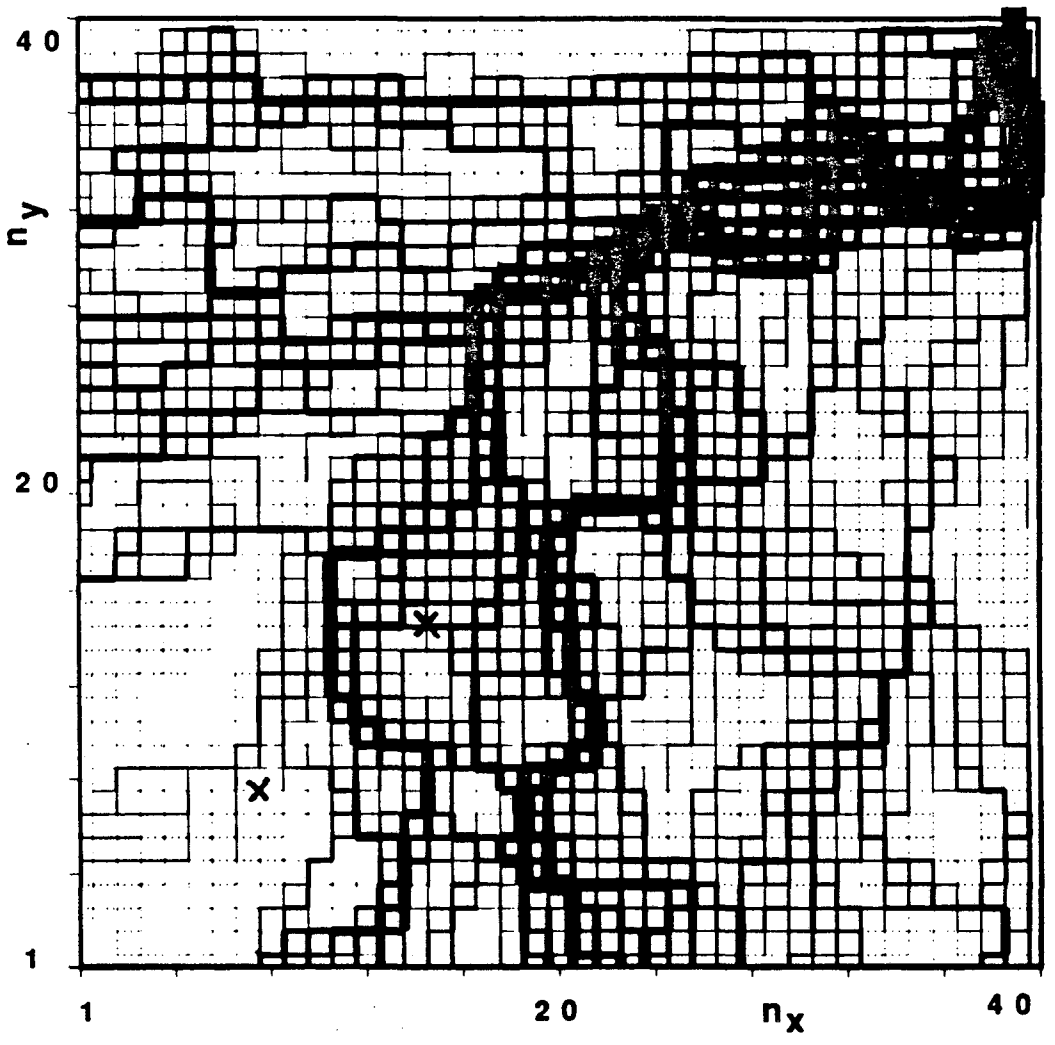

Figure 6 Flow paths in fracture 2 for a negligible injection flowrate. The injection points ("x") are (15,15) and (8,8).

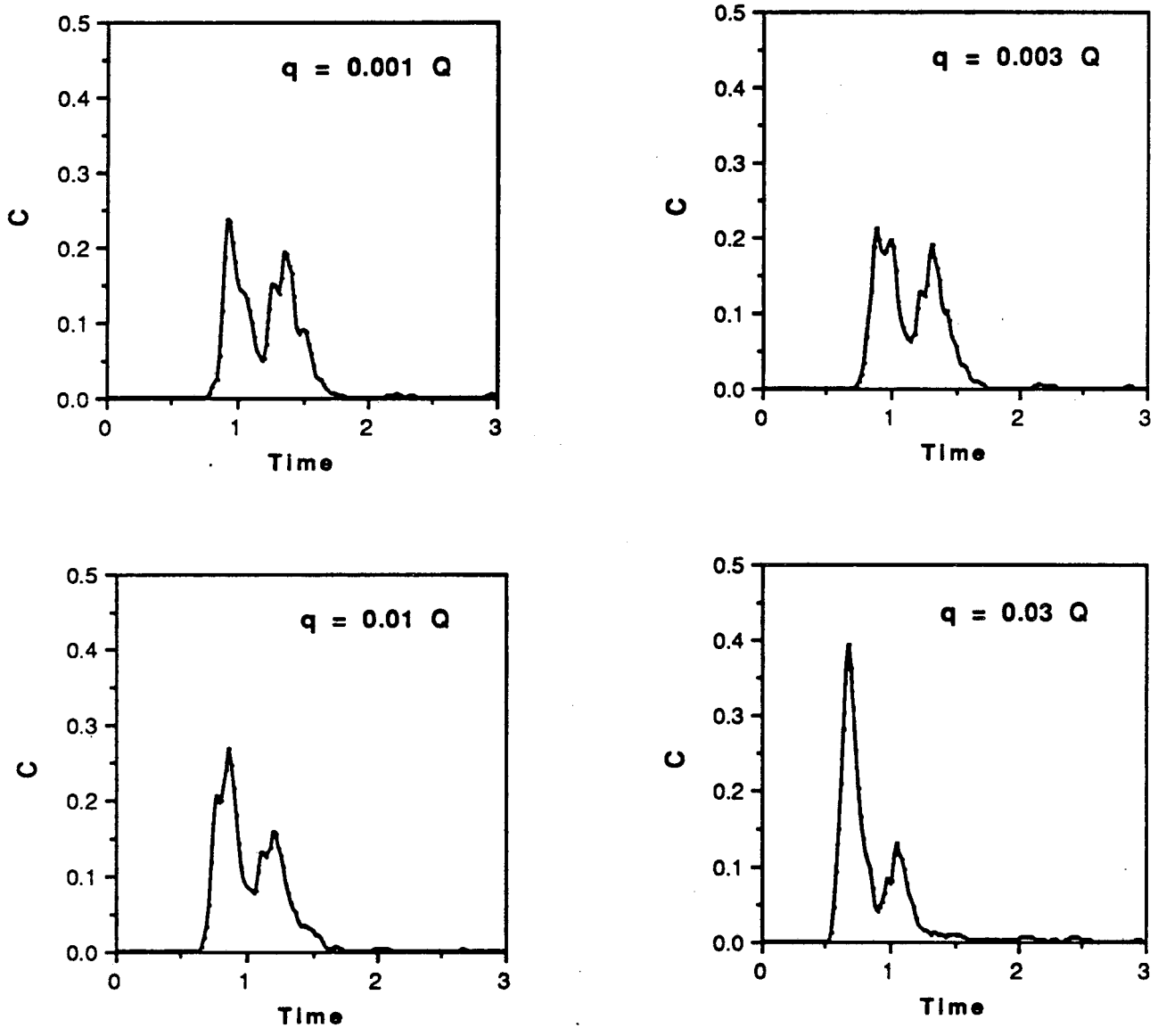

Figure 7 Breakthrough curves for fracture 2, for injection flowrate of 0.001 Q, 0.003 Q, 0.01 Q, and 0.03 Q. Injection at (8,8).

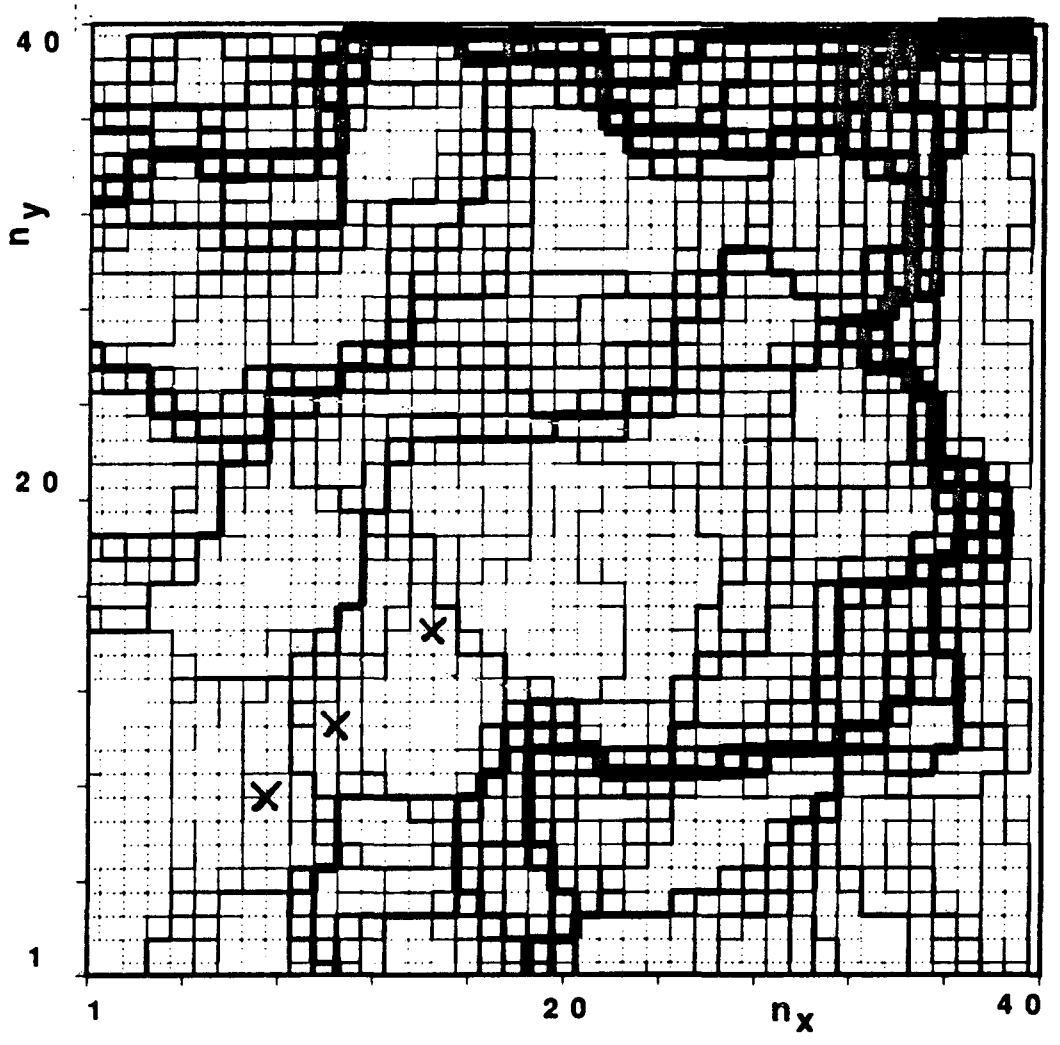

Figure 8 Flow paths in fracture 3 for a negligible injection flowrate. The injection points ("x") are (15,15), (11,11), and (8,8).

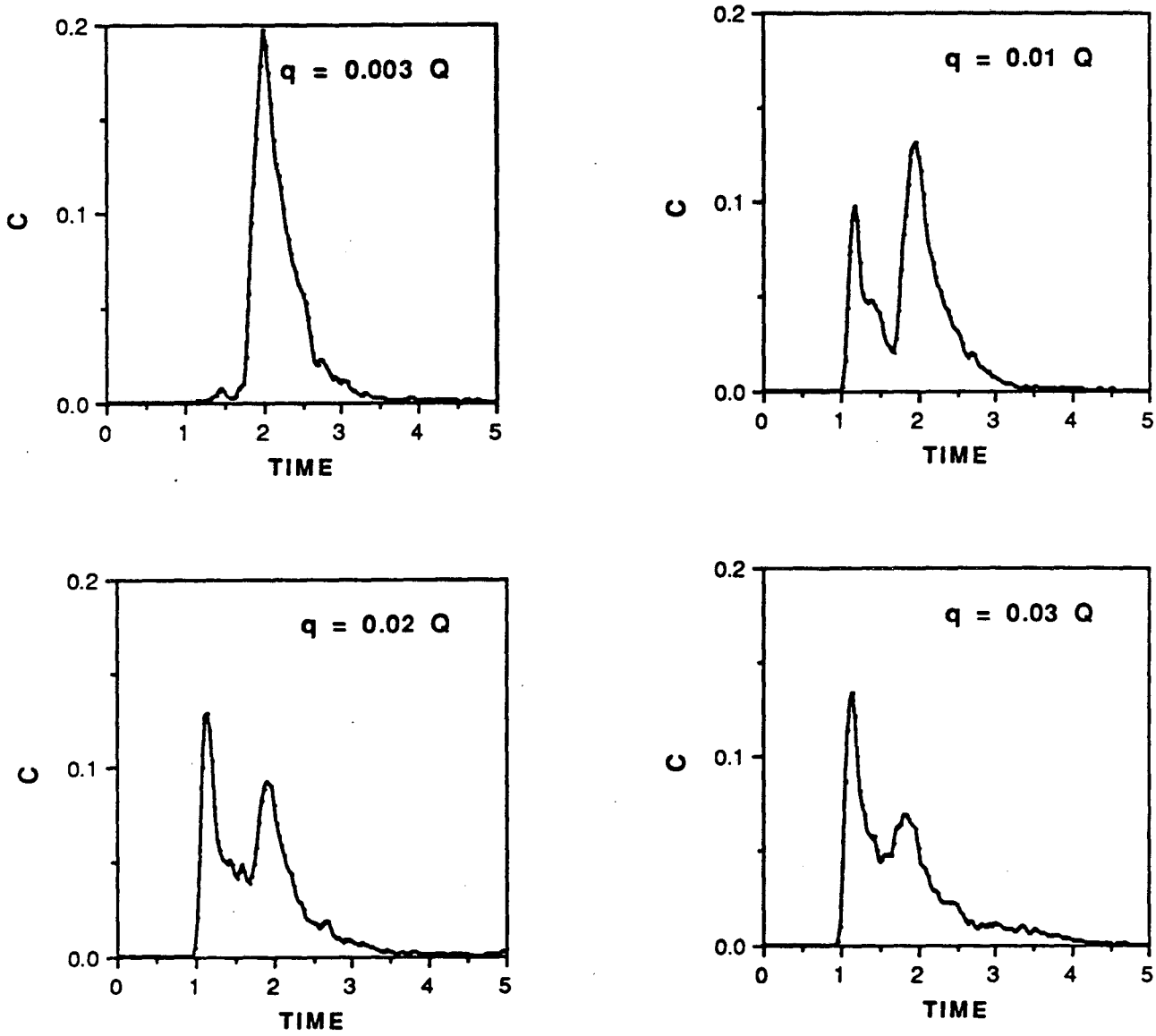

Figure 9 Breakthrough curves for fracture 3, for injection flowrate of 0.003 Q, 0.01 Q, 0.02 Q, and 0.03 Q. Injection at (8,8).

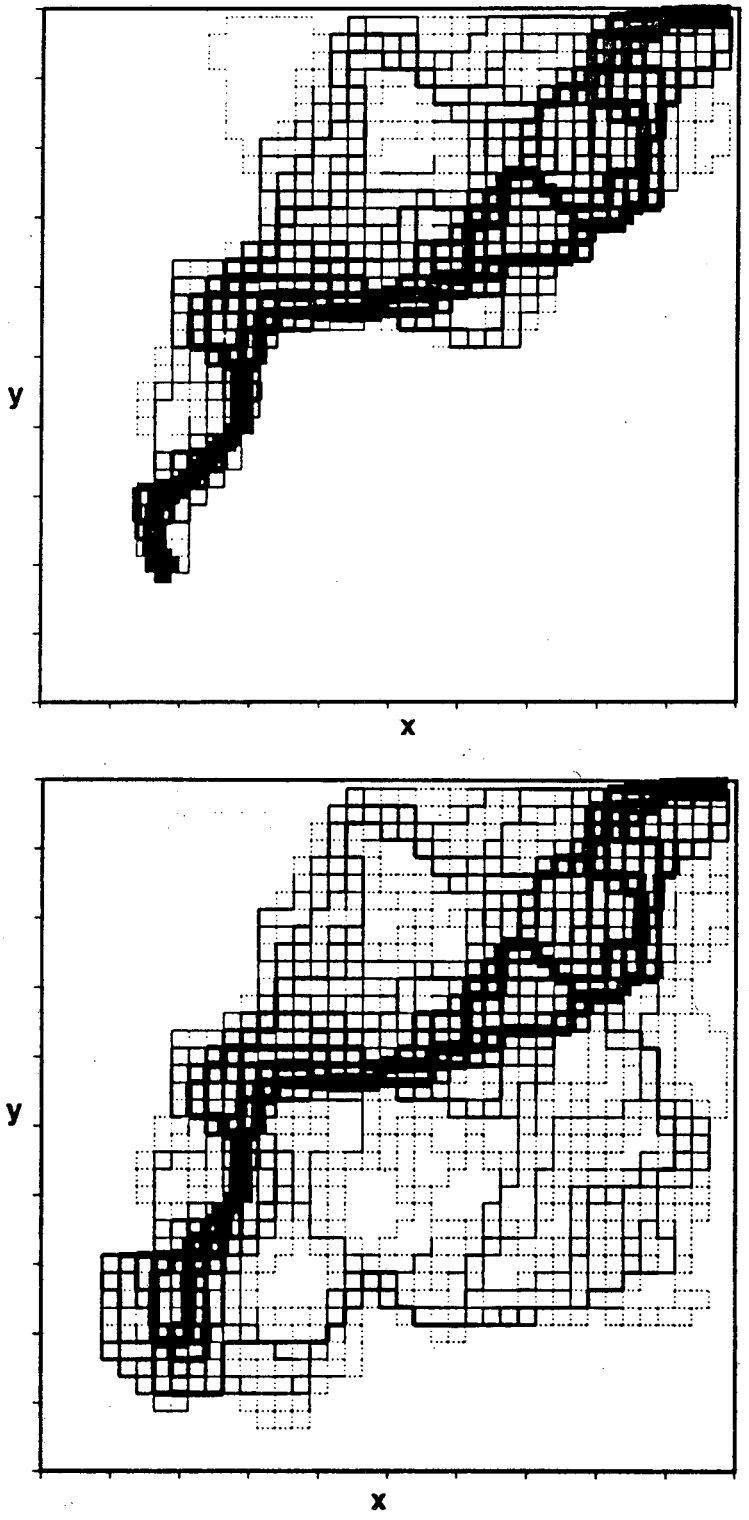

Figure 10 Tracer paths in fracture 3 for injection flowrate of 0.003 Q and 0.03 Q. Injection at (8,8).

LAWRENCE BERKELEY LABORATORY
UNIVERSITY OF CALIFORNIA
INFORMATION RESOURCES DEPARTMENT
BERKELEY, CALIFORNIA 94720